Review Article

Externally modulated theranostic nanoparticles

Cordula Urban[1], Alexander S. Urban[2], Heather Charron[1], Amit Joshi[1]

[1]Department of Radiology, Baylor College of Medicine, Houston, TX, USA; [2]Electrical and Computer Engineering, Rice University, Houston, TX, USA

Corresponding to: Amit Joshi. Department of Radiology, Baylor College of Medicine, Houston, TX, USA. Email: amitj@bcm.edu.

Abstract: Externally modulated nanoparticles comprise a rapidly advancing class of cancer nanotherapeutics, which combine the favorable tumor accumulation of nanoparticles, with external spatio-temporal control on therapy delivery via optical, magnetic, or ultrasound modalities. The local control on therapy enables higher tumor treatment efficacy, while simultaneously reducing off-target effects. The nanoparticle interactions with external fields have an additional advantage of frequently generating an imaging signal, and thus such agents provide theranostic (both diagnostic and therapeutic) capabilities. In this review, we classify the emerging externally modulated theranostic nanoparticles according to the mode of external control and describe the physiochemical mechanisms underlying the external control of therapy, and illustrate the major embodiments of nanoparticles in each class with proven biological efficacy: (I) electromagnetic radiation in visible and near-infrared range is being exploited for gold based and carbon nanostructures with tunable surface plasmon resonance (SPR) for imaging and photothermal therapy (PTT) of cancer, photochemistry based manipulations are employed for light sensitive liposomes and porphyrin based nanoparticles; (II) Magnetic field based manipulations are being developed for iron-oxide based nanostructures for magnetic resonance imaging (MRI) and magnetothermal therapy; (III) ultrasound based methods are primarily being employed to increase delivery of conventional drugs and nanotherapeutics to tumor sites.

Key Words: Cancer nanotechnology; theranostics; hyperthermia; NIR therapy; gold nanoparticles (AuNPs)

Submitted Jul 15, 2013. Accepted for publication Aug 20, 2013.
doi: 10.3978/j.issn.2218-676X.2013.08.05
Scan to your mobile device or view this article at: http://www.thetcr.org/article/view/1548/2263

Introduction

Nanoparticles sized in the range of 10-500 nm are rapidly advancing for imaging and therapy of cancer. Nanoparticles are larger in size than proteins and macromolecules constituting the cells, but much smaller than typical cells, and are comparable to subcellular structures, such as ribosomes. Thus, they exhibit different pharmacokinetic and pharmacodynamic properties than conventional small molecule therapeutic agents. Specifically, they can escape renal clearance mechanisms and are frequently engineered to escape the reticuloendothelial system (RES)-based clearance from plasma by stealth coatings (1). The ensuing long circulation time enables efficient trapping in the leaky vasculature of tumors, and provides the motivation for using nanoparticles as tumor targeted diagnostic and therapeutic agents. The early phase of therapeutic cancer nanotechnology research focused on the development of passive nanocarriers, such as liposomes, micelles, polymeric NPs, dendritic NPs, and silica (SiO_2) NPs (2,3), for delivering chemotherapy payloads to tumors sites. These nanocarriers can be molecularly targeted to specific tumor types, but internal tissue processes for nanoparticle degradation govern release of drug payload or therapeutic action, and no external control is exercised on therapy delivery after the nanoparticle injection. For further enhancement of therapy specificity to disease sites, and to reduce off-target effects, direct spatial and temporal control on therapy delivery is desirable. Parallel developments in biomedical imaging and engineering fields have led to technologies for interrogating tissue with electromagnetic, sonic, and magnetic energy fields. Combining the advances

© Pioneer Bioscience Publishing Company. All rights reserved.

Table 1 Externally modulated theranostic nanoparticles

External control modality	Nanoparticle	Development stage
Light/RF/Other electromagnetic radiation	Solid gold/Silver/Platinum nanospheres	Pre-clinical
	Gold nanorods	Pre-clinical
	Gold nanoshells	Clinical trial
	Light sensitive liposomes	Pre-clinical
	Carbon nanotubes	Pre-clinical
	Porphysomes	Pre-clinical
Heat	Heat sensitive liposomes ($HER2^+$ affisomes)	Pre-clinical
Magnetic field	Superparamagnetic iron-oxide nanoparticles (SPIONs), Iron core-iron oxide nanoparticles	Pre-clinical
Ultrasound	Drugs encapsulated into polymeric micelles	Pre-clinical

in nanoparticles and biomedical engineering has led to the emergence of nanoparticles, which are sensitive to external electromagnetic, sonic, or magnetic fields and employ these interactions to deliver a local therapeutic action. Further, these nanoparticles typically combine diagnostic and therapeutic features, and are referred to as theranostic nanoparticles, as the sensitivity to external fields can be directly employed for imaging with optical, MR, or ultrasound modalities. In this review we briefly summarize the recent developments in the field of cancer nanotechnology related to externally modulated theranostic nanoparticles. The following sections are organized in terms of mode of external control of nanoparticle therapy: electromagnetic (visible and NIR light), magnetic fields, and sonic energy. Leading nanoparticle embodiments for each mode are then described with reported *in vivo* applications for cancer therapy. The external modalities and associated nanoparticles are summarized in *Table 1*.

Therapeutic nanoparticles modulated with light

Electromagnetic radiation in visible, near-infrared, and longer wavelengths is an attractive source for transferring energy to living tissue, due to its non-ionizing nature. The most common therapeutic method modulated with light is hyperthermia or photothermal therapy (PTT). Since ancient times heat has been used for cancer therapy, one of the first treatment methods being the glowing tip of an iron rod, which was used to treat breast cancer (4). Radio frequency, microwaves, ultrasound or laser irradiation are now used to induce heat in a specific target area or tissue (5). Nanoparticles can enhance the photothermal efficacy significantly by virtue of their high accumulation in tumors, and by suitable design, which allows the engineering of high optical absorption cross-sections. A second light triggered therapeutic modality is photodynamic therapy (PDT), which relies on photo-chemistry based generation of singlet oxygen for cell death. Recently nanoparticles relying on photochemistry for releasing drug payloads, or direct PDT have been proposed. In the following sections, we describe the major classes of light triggered nanoparticles for photothermal and photodynamic therapies.

Gold nanoparticles (AuNPs)

Noble metal nanoparticles show unique tunable optical properties because of their surface plasmon resonance (SPR). The plasmon, a quasiparticle, can be described as a coherent oscillation of the free electron density with respect to the stationary ions in a metal. Surface plasmons occur at the interface between a metal and a dielectric and interact strongly with light, in the case of metallic nanoparticles these are known as localized surface plasmons (LSP). When a photon impinges on a nanoparticle an LSP is created, which can decay radiatively by emission of photons (scattering) or nonradiatively by electron-hole excitations (absorption) (6). These thermalize quickly through phonon scattering with the ion lattice, resulting in a heating of the nanoparticle, which can thus reach extremely high temperatures (7,8). The resonance position of the plasmon depends strongly on the material of the nanoparticle, lying anywhere between the UV (aluminum) (9), blue (silver) (10), green (gold), red (copper) (11) and infrared (highly doped semiconductors) (12). Additionally, the size and shape of the nanoparticles play a huge role on the position of the resonance as does the refractive index of

© Pioneer Bioscience Publishing Company. All rights reserved.

the surrounding medium.

Plasmonic PTT, the specific use of noble metal nanoparticles, commonly focusing on gold, to convert externally applied light/laser energy into heat within a specific tissue, has been investigated in several studies.

AuNPs absorb light at their plasmon resonance, which lies in the visible range of the spectrum, and convert this light highly efficiently into heat. This heat is confined to the immediate vicinity of the nanoparticle and thus can be applied highly locally to specific regions of tissue. Because of their strong SPR enhanced absorption the use of noble metal nanoparticles decreases the laser power needed to achieve hyperthermia within the tumor tissue to achieve irreversible tissue damage (13). Additionally, the scattering properties of the AuNPs allow for them to be used as optical and spectroscopic tags for biological sensing, imaging or for therapy (14). The surface of gold has an extremely high affinity for thiol groups or amines, enabling the nanoparticles to be pegylated, i.e., modified with poly-ethylene-glycol (PEG) for better biocompatibility (15), with antibodies for a more specific biodistribution or with dyes for improved imaging properties (16,17). Due to the low reactivity of gold, resulting in a low cell toxicity, the AuNPs are a perfect tool for nanomedical applications (18). Although individual studies have demonstrated cell toxicity through reactive oxygen production, apoptosis, cytokine release or necrosis (19-21), most studies show no cell toxicity induced by the use of AuNPs. Depending on the size and shape of the nanoparticles laser energy at a specific wavelength is needed to conduct the hyperthermia treatment. Pure gold nanospheres ranging in size from 20 to 80 nm show their plasmonic peak in the visible range of 520 to 580 nm whereas the plasmonic peak of nanoshells or nanorods can be shifted into the near-infrared window. The near-infrared window, where the human tissue has its highest transmissivity (22) shows best conditions for clinical therapy applications, where tumors often lie deep inside the body.

Solid spherical AuNPs

The simplest form of AuNPs are spherical nanoparticles, which have been produced for over 50 years (23-25), and by now are easy to fabricate in large size ranges, with high yields and low size and shape dispersity (26). Spherical gold NPs used for cancer therapy are often around 20-30 nm in diameter (27-29). In this size range, the nanoparticles absorb a strong amount of light in the range of 520-530 nm and convert this nearly entirely into heat. Both continuous wave (cw) and pulsed lasers have given promising results for PTT in studies. Afifi *et al*. 2013 (27) used 30 nm spherical AuNPs to treat hamster buccal pouch carcinoma (HBP) and to investigate the short-term effect of plasmonic PTT on the HBP. Nanoparticles and cancer cells were injected simultaneously in Syrian male hamsters. The treatment was conducted with a cw laser diode at 532 nm wavelength (150 mW, 8 mm spot size diameter). Treated animals showed a decrease in tumor growth, meaning this might be applicable for cancer treatment in humans. Mendoza-Nava *et al*., 2013 (28) used 20 nm AuNPs functionalized with ocreotide in an *in vitro* experiment with HeLa cells. The treatment was conducted using an Nd:YAG laser with 5 ns pulses at 532 nm with a repetition rate of 10 Hz for 6 min (0.65 W/cm^2). The results in this experiment hint at a possible usage for plasmonic PTT of cervical cancer. Li *et al*., 2009 (21) also used a pulsed laser (530 nm, various power densities, 1ns pulse length, repetition 10 Hz for 5 min) for the *in vitro* PTT of ductal carcinoma cells.

The main problem of using small spherical gold NPs for PTT lies in the position of the resonance peak which, depending on the size of the nanoparticle, is located between 520 and 580 nm (13). But in this wavelength range healthy tissue, specifically hemoglobin and oxygenated hemoglobin (30), strongly absorbs light and converts the light energy into heat. Thus, healthy tissue can also be damaged during the PTT, making spherical nanoparticles less ideal for PTT.

Gold nanorods (GNRs)

The so-called biological NIR window is a region in the optical spectrum between 650 and 900 nm, in which the absorption of light inside tissue is minimal due to both low absorption of hemoglobin and water. One of the first AuNPs shown to have a plasmon resonance in this region is the nanorod, first synthesized in the mid-90s (31) and refined in 2001 (32). Due to their elongated shape, with the short axes being around 10-45 nm and the long axis around 50 to several hundred nanometers, the LSP band of the nanorods is split into two modes, a transverse mode (along the short axes) and a longitudinal mode (along the long axis), which is by far the stronger of the two (33,34). The resonance position of the longitudinal mode is tunable by modifying the aspect ratio, which is the ratio of the long to short axis dimensions of the nanorod. Thus the plasmon resonance of the nanorod can be tuned easily throughout the NIR region (35,36). In 2006 Huang *et al*. (37) showed for the first time the use of GNRs for PTT applications in cancer treatment (*Figure 1*). Like the spherical AuNPs,

© Pioneer Bioscience Publishing Company. All rights reserved.

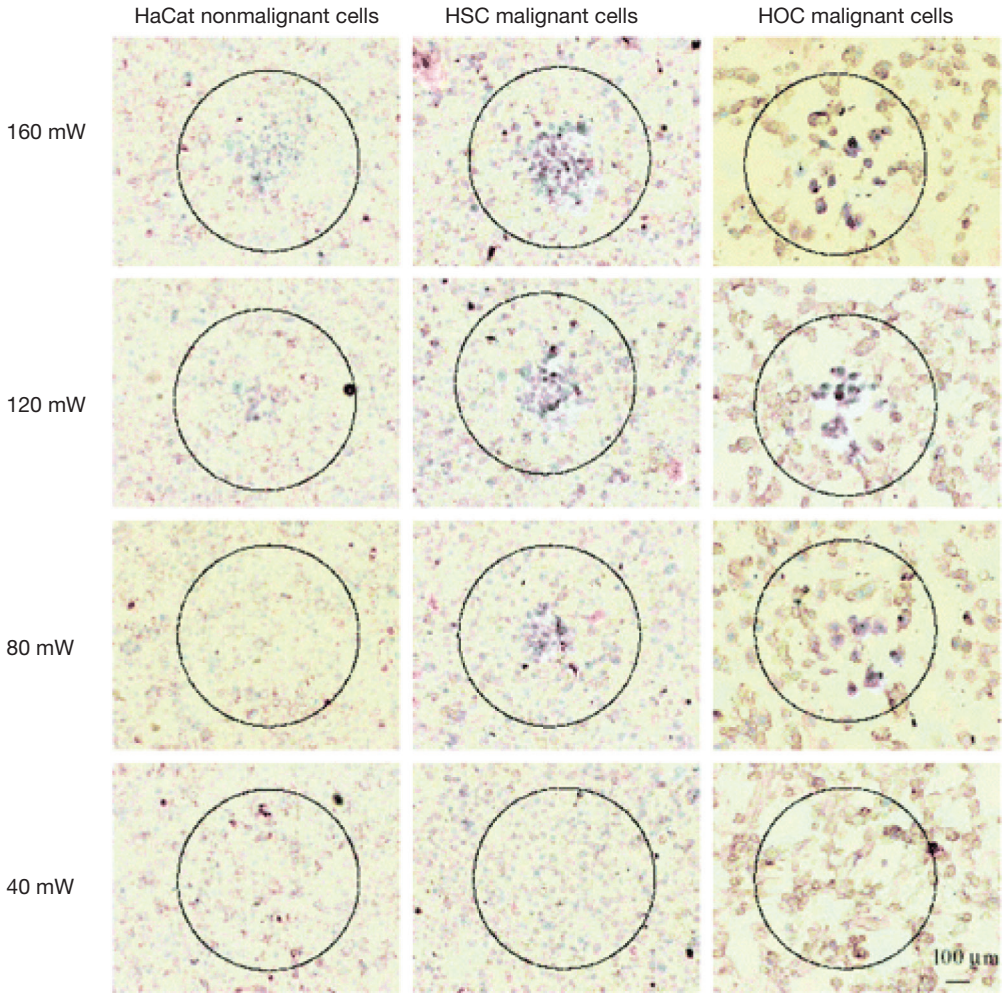

Figure 1 Selective photothermal therapy of cancer cells with anti-EGFR/Au nanorods incubated. The circles show the laser spots on the samples. At 80 mW (10 W/cm^2), the HSC and HOC malignant cells are obviously injured while the HaCat normal cells are not affected. The HaCat normal cells start to be injured at 120 mW (15 W/cm^2) and are obviously injured at 160 mW (20 W/cm^2) [Reproduced with permission (37), Copyright © American Chemical Society, 2006]

GNRs are also easy to modify with antibodies, biomolecular ligands or other targeting molecules. All the different properties of the GNRs have been investigated for cancer medicine like imaging, diagnostic and potential therapy and different combinations of properties like imaging and therapy with the same particle (38-40).

In a promising *in vitro* experiment using GNR-antibody conjugates with an aspect ratio of 3.9 and the SPR overlapping with the cw Ti:Sapphire red laser wavelength at 800 nm, malignant and normal cells were incubated with the GNRs and then treated with the laser for 4 min. Using 160 mW (20 W/cm^2) malignant and normal cells were both killed. An antibody was conjugated to the GNR, targeting a receptor, which is overexpressed on the membranes of the malignant cells. The GNRs accumulated much more on the malignant cells than on normal cells; and by reducing the laser power to 80 mW (10 W/cm^2) the malignant cells were killed while the normal cells didn't show any sign of damage (33).

Two different ways of applying pegylated GNRs (GNR-PEG) in a mouse model were described by Dickerson *et al.*, 2008 (18). In the first method, the GNR-PEG was injected directly into the tumor, which was irradiated within 2 min after injection to avoid particle diffusion beyond the tumor boundaries. The tumors were exposed to a cw diode laser at 808 nm, with 0.9-1.1 W/cm^2 power density and a

© Pioneer Bioscience Publishing Company. All rights reserved.

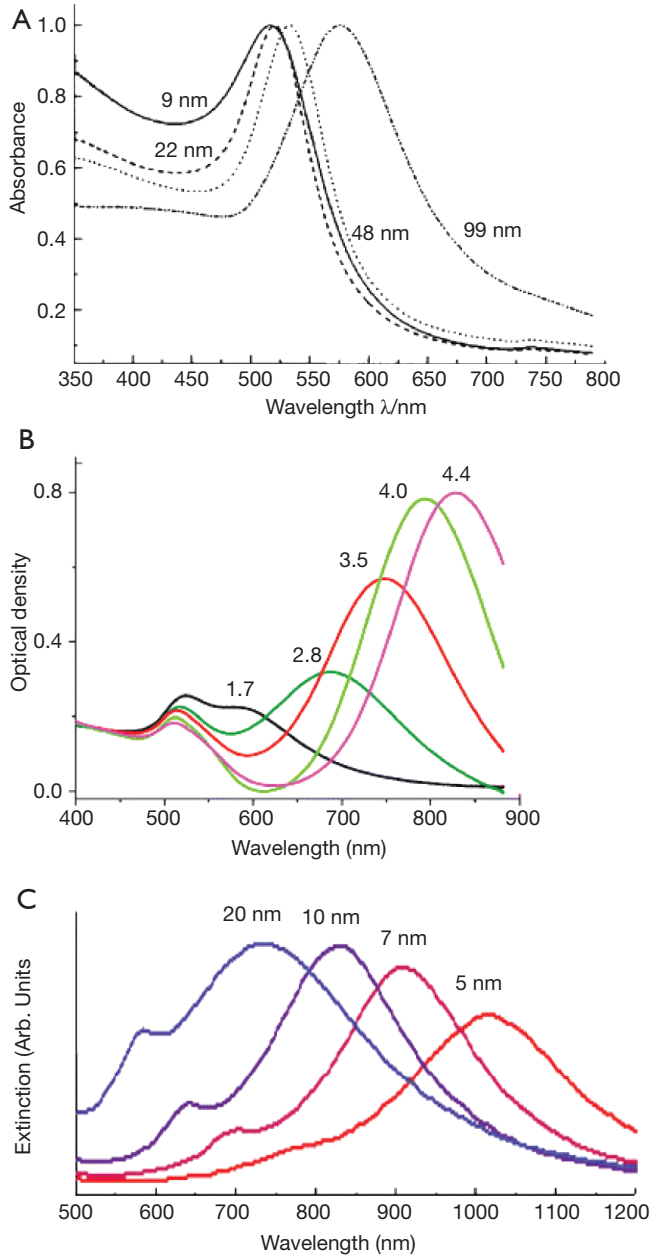

Figure 2 Size, shape, and composition dependence of the surface plasmon absorption spectrum of plasmonic gold nanostructures. A. nanospheres of different sizes [Reproduced with permission (50), Copyright © American Chemical Society, 1999]; B. nanorods of different aspect ratios [Reproduced with permission (51), Copyright © American Chemical Society, 2003]; C. nanoshells of different shell thicknesses [Reproduced from (47), open access article]

6 mm diameter spot, for 10 min. The second application method involved injecting the GNR-PEG into the tail vein for a systemic administration in the body. A circulation time of 24 hours was given to maximize the particle uptake and accumulation within the tumor. Tumors then were exposed to the same laser settings but with a different power density: 1.7-1.9 W/cm^2. Both delivery groups showed an inhibition in tumor growth over a period of two weeks. The directly-injection method, with a tumor reduction of around 57% compared to 25% for the distribution method, was more than twice as successful in reducing the tumor size. All of these reviewed experiments with GNRs are very promising for clinical application in cancer therapy.

However, GNRs do have a drawback. Despite a very high bulk melting temperature of gold (1,064 ℃), GNRs can undergo rapid reshaping through surface diffusion of gold atoms at temperatures below 200 ℃. This process occurs on the order of hours; and for temperatures greater than 250 ℃, the rods are completely transformed into spheres within a matter of minutes. The reshaping is quantified by monitoring UV-VIS spectra of nanorod solutions. As the rods reshape, their aspect ratio is reduced, which leads to a strong blueshift of the longitudinal nanorod resonance (41). This reshaping can also occur during laser irradiation of the nanorods, provided that the laser pulses are long enough. For ultrafast excitation of the nanorods, the cooling time is much too fast to allow for a diffusion of the gold atoms, even up to temperatures of 700 ℃ (42,43). That's why it is difficult or even impossible to do more than one treatment cycle with GNR in contrast to nanospheres or nanoshells, which don't change their shape even after a long or high power laser irradiation (44,45).

Gold nanoshells (GNS)

GNS were the first nanoparticles demonstrated to have a use in PTT for cancer (46-48) and the translation into clinical trials is currently underway (49).

GNS, approximately 100-160 nm in diameter, consist of an inner SiO_2 core and a thin outer layer of gold. Depending on the core-shell ratio the SPR is easily tunable throughout the near-infrared window (*Figure 2*). They accumulate in tumors due to the leaky vasculature and the enhanced permeability and retention (EPR) effect of tumor tissue (52). Like other AuNPs, GNS are also easy to modify so they can be used simultaneously for diagnostics, imaging and PTT. The number of particles delivered to the tumor is highly correlated with the radius of the particles, with a larger radius leading to a decreased delivery of the GNS (53). Gad *et al.*, 2012 (54) could show in a huge evaluation, testing for pyrogenicity, genotoxicity, *in vitro* hemolysis, intracutaneous reactivity, sensitization or

© Pioneer Bioscience Publishing Company. All rights reserved.

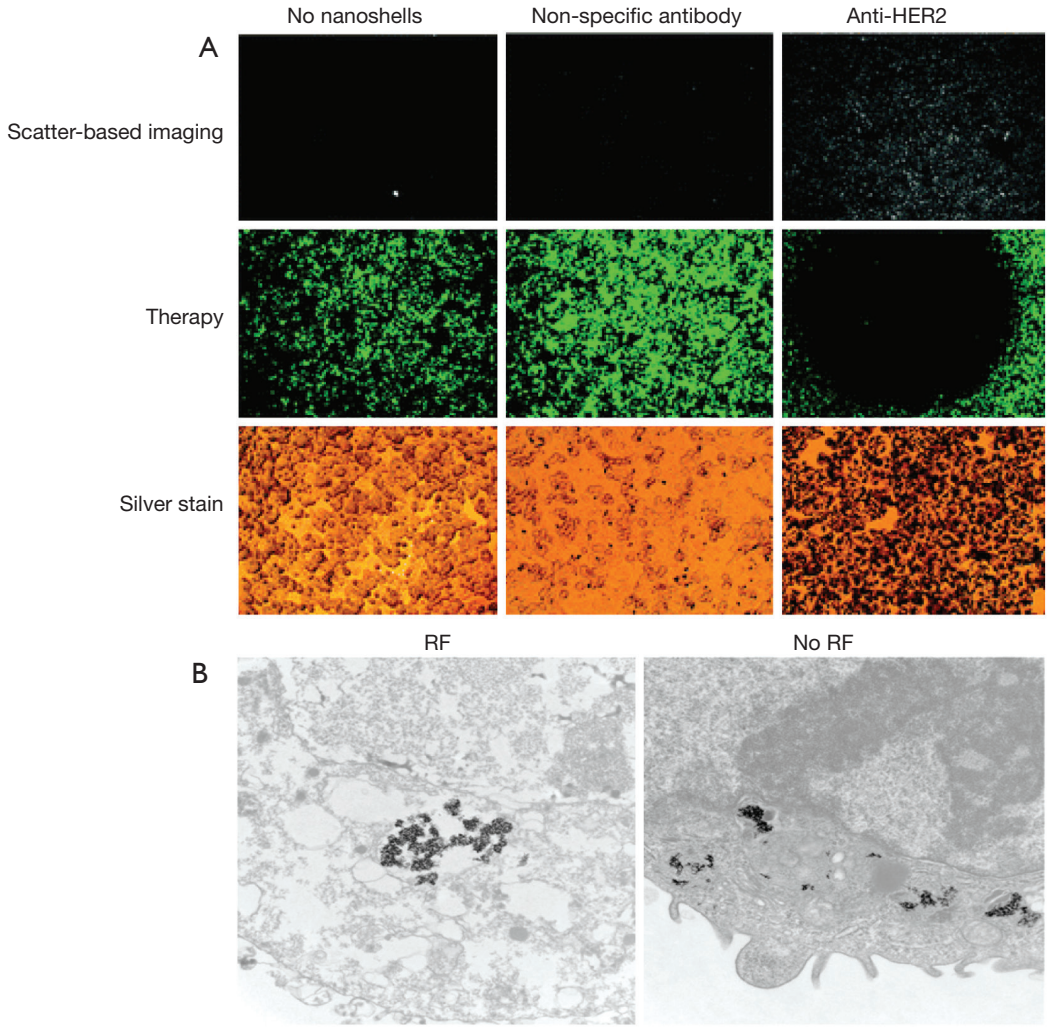

Figure 3 A. Combined imaging and therapy of SKBr3 breast cancer cells using HER2-targeted nanoshells. Scattering-based darkfield imaging of HER2 expression (top row), cell viability assessed via calcein staining (middle row), and silver stain assessment of nanoshell binding (bottom row). Cytotoxicity was observed in cells treated with a NIR-emitting laser following exposure and imaging of cells targeted with anti-HER2 nanoshells only. Note increased contrast (top row, right column) and cytotoxicity (dark spot) in cells treated with a NIR-emitting laser following nanoshell exposure (middle row, right column) compared to controls (left and middle columns), [Reproduced with permission (55), Copyright © American Chemical Society, 2005]; B. Transmission electron microscopy of Panc-1 cells treated with 67 μM gold gold nanoparticles. Panel 1, 2 minutes of external radiofrequency (RF) field treatment. Note loss of nuclear stability and prominent vacuolization; Panel 2, No RF treatment. Nuclear integrity and normal appearing organelles [Reproduced from Reference (56), Open Access Article]

systemic toxicity that 150 nm GNS conjugated with PEG did not show any kind of toxicity at all. Even in long term *in vivo* studies over 404 days no toxicity or bioincompatibilities were identified.

Hirsch *et al*., 2003 (46) used GNS for magnetic resonance guided near-infrared PTT. *In vitro* tests with human breast carcinoma cells, which were incubated with the GNS and then irradiated with an 820 nm cw NIR-laser (35 W/cm^2) for 7 minutes, showed irreversible cell damage on the cells whereas control cells, also irradiated with the same power but not incubated with GNS, showed no cell damage (*Figure 3*). *In vivo* tests with the same GNS in tumor bearing mice had similar results: GNS injected directly into the tumor tissue and irradiated with an 820 nm cw NIR-laser (4 W/cm^2)

© Pioneer Bioscience Publishing Company. All rights reserved.

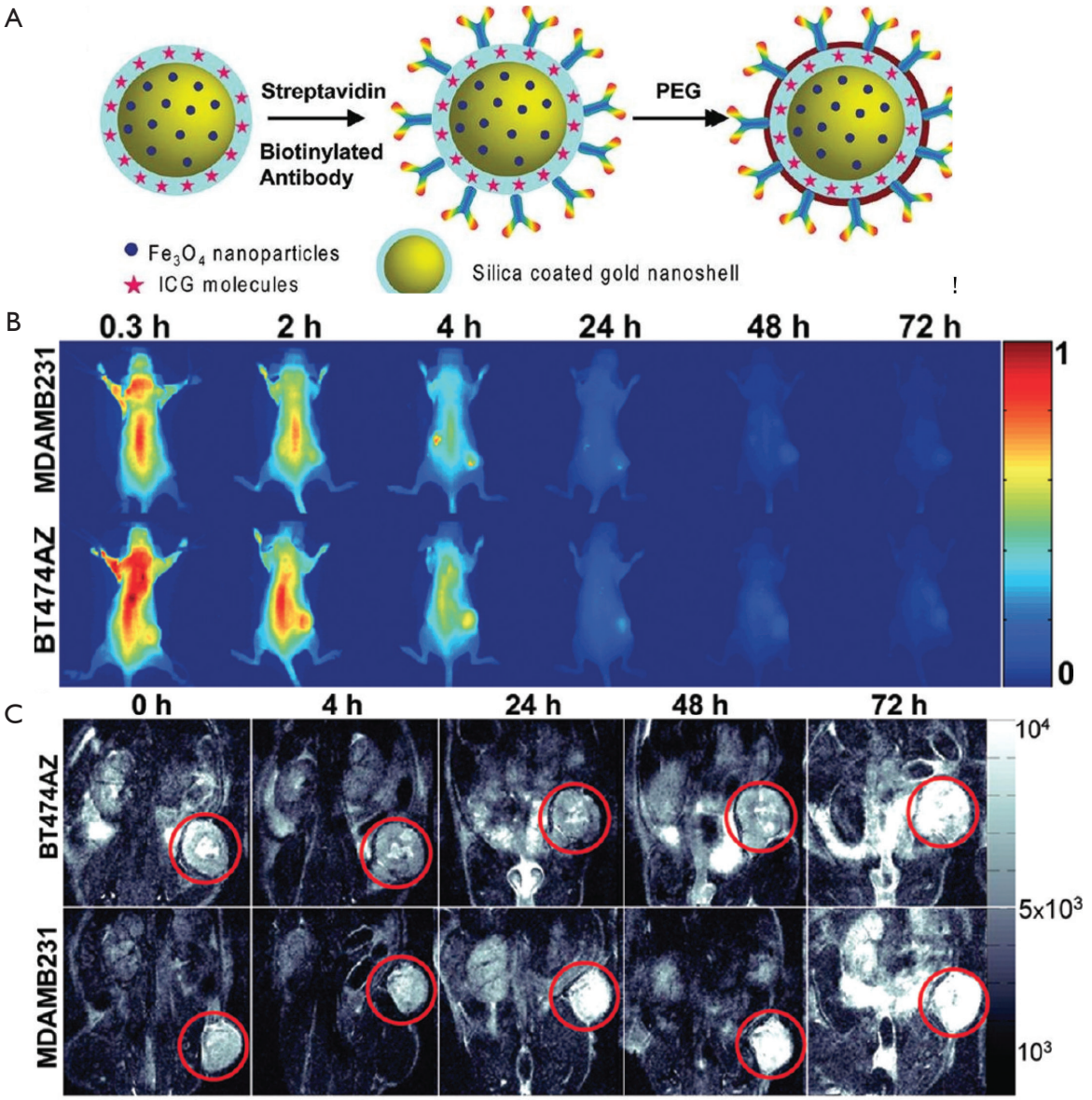

Figure 4 A. Schematic representation of antibody and PEG conjugation to nanocomplexes; B. Time dependent fluorescence images of mice injected with magneto-fluorescent nanoshells; C. Corresponding MR images of the same mice [Reproduced with permission (16), Copyright © American Chemical Society, 2010]

for 6 minutes induced irreversible tissue damage but no damage in the control tumor, because the temperature increase in the control tumor wasn't sufficient enough to induce irreversible tissue damage. Bardhan *et al*., 2010 (16) used multimodal GNS, incorporated with iron oxide (Fe_3O_4) for magnetic resonance imaging (MRI) (57), indocyanine green (ICG) on the surface as near-infrared fluorophore, PEG for a better biocompatibility and antibodies for higher and more specific biodistribution and uptake into the tumor (*Figure 4*). Biodistribution studies showed the selective uptake in the tumor and the stability of the particles which provide all the properties needed for early cancer diagnostics and therapy. Similar particles were used in an *in vitro* experiment (57), where human epidermal growth factor receptor (HER2)-overexpressing human breast cancer cells were compared to HER2-negative ($HER2^-$)

© Pioneer Bioscience Publishing Company. All rights reserved.

breast cancer cells. Both cell types were incubated with the multimodal nanoparticles and then irradiated with an 808 nm cw laser (3.72 W/cm^2, 1mm diameter spot size) for 10 min. The HER2-expressing (HER2$^+$) cells showed a higher rate of cell death than the HER2$^-$ cells due to the specificity of the HER2-targeting antibodies.

The simultaneous use of GNS for diagnostics, imaging and therapy, also known as *theranostics*, has made progress and will make significant more progress within the next years. But there is still one disadvantage of using GNS for PTT or theranostics. Since August 2002 a US patent exists that regulates the use of GNS for theranostic purposes (58), that means it is not completely free and easy to do research with GNS as with, e.g., GNR. But on the other hand GNS in contrast to GNR are highly stable due to their shape and composition. Even after several rounds of PTT they do not change their shape or properties (44,45).

Other gold/silver nanoparticles

While GNRs and nanoshells have undergone most progress towards clinical translation, plasmonically active noble metal nanoparticle development is an active area, with a particular research focus on sub 100 nm gold nanostructures, which retain NIR resonance. PTT has been successfully demonstrated with many near-IR absorbing gold nanostructures including branched nanoparticles (59), nanohexapods (60), nanocages (61,62), and hollow GNS (63,64). The physical principles and laser powers employed for photothermal treatment required for these nanoparticles are similar to those involved in nanorod or nanoshell guided treatments described in the previous sections.

Light sensitive liposomes

Liposomes are increasingly being used as nanocarriers for pharmaceuticals. Liposomes are primarily comprised of phospholipids. Depending on their phospholipid composition the properties of the liposomes are tunable. By adding cholesterol into the liposomes, the melting temperature of the liposome, which is the temperature at which the phospholipids undergo a transition into the liquid crystalline phase, can be set to a specific temperature (65,66). At this temperature the membrane is destabilized, and the content of the liposome, e.g., cancer chemotherapeutics such as Doxorubicin (DOX), can be released. Another way to make the liposomes "triggerable" is by using a light-sensitive phospholipid composition. Exposure to light with a certain wavelength can lead to the photo-polymerization of the light-sensitive component resulting in the formation of chains of covalently linked lipid molecules in the bilayer. The creation of the phase boundary defects in the membrane causes a higher membrane permeability resulting in the release of the liposome content (67-70). By modifying the liposomes with targeting ligands, e.g., with antibodies, the liposomes are also able to accumulate specifically in the desired tissue (71). The targeting potential and the triggering (on-demand drug release) are essential for the translation into clinical trials. Doxil, liposomal delivered DOX, is one of the first nanoparticles to be approved by FDA for patient care.

Smith *et al*., 2011 (72) used heat-sensitive liposomes with modified HER2-affisomes (HER2$^+$ affisomes). Affibody® affinity ligands are innovative protein-engineering technologies (73). The liposomes were either loaded with rhodomine-PE and calcein or with Dox. HER2$^+$ cells and HER2$^-$ cells were both incubated with the liposomes. Flourescently labeled HER2$^+$ affisomes showed a 10-fold higher increase in binding to HER2$^+$ cells compared to the binding to HER2$^-$ cells. After incubation with a 45 ℃ buffer for 20 min a substantial calcein release was detected in the cytosol of the cells. Compared to control liposomes the HER2$^+$ affisomes also showed, after incubation at 45 ℃ for 20 min, a 2-3 higher accumulation of DOX in the cells and therefore a higher DOX-mediated cytotoxicity, even after incubation with lower doses of HER2$^+$ affisomes.

Yavlovich *et al*., 2010 (74) worked on light sensitive liposomes. They compared different lipid combinations and formulations of DPPC (1,2-Dipalmitoyl-*sn*-Glycero-3-Phosphocholine) and the phototriggerable $DC_{8,9}PC$ [1,2-bis(tricosa-10,12-diyonyl)-*sn*-Glycero-3-Phosphocholine]. Exposure to a UV lamp with 254 nm for up to 40 min resulted, depending on the liposome formulation, in almost 80% release of the encapsulated calcein. No calcein release was observed when the control liposomes without $DC_{8,9}PC$ were treated under the same conditions, demonstrating that $DC_{8,9}PC$ can be used as a light sensitive component in drug carrier liposomes.

These two exemplary experiments give eligible hope that both light and heat triggerable liposomes have the potential to be used in cancer treatment. But further investigations need to be carried out to translate these results into *in vivo* applications.

Carbon nanoparticles

Carbon nanotubes are allotropes of carbon of the fullerene structural family, with extraordinary thermal conductivity,

© Pioneer Bioscience Publishing Company. All rights reserved.

mechanical stability and electrical properties. Their structure is comprised of a graphene sheet rolled at specific and discrete angles. The combination of angles and radii determine the nanotube properties, e.g., whether a nanotube has metallic or semi-conductor properties. A multi-walled nanotube (MWCNTs) consists of many concentric layers of single-wall nanotubes (SWCNTs). As predicted in classical antenna theory optical coupling is most efficient for a nanotube length of at least half the wavelength of the applied laser (75). MWCNTs show an extraordinarily long dephasing time. That means that the currents travel essentially without scattering, resulting in a giant oscillator strength material, or a "super-antenna" (76). MWCNTs release substantial vibrational energy after exposure to near-infrared irradiation. The energy within the tissue produces localized heating which can potentially be used for cancer treatment. Compared to SWCNTs, MWCNTs can be expected to absorb significantly more near-infrared irradiation because MWCNTs have more available electrons for absorption per particle. This will reduce the amount of irradiation needed for successful cancer treatment which also reduces damage in the surrounding tissue (76,77).

Burke *et al*., 2009 (78) demonstrated that MWCNTs can be used to treat kidney tumor-bearing mice. A 1,064 nm cw laser was used to treat the tumors. One single short 30-sec treatment with low laser power (3 W/cm^2) was enough to result in a complete ablation of the tumor and a >3.5-month durable remission in 80% of the mice. Only a minimal local but no systemic toxicity was observed. Fisher *et al*., 2010 (79) showed in their study that MWCNTs, irradiated with appropriate laser settings, induce a significant temperature increase within human and murine cells that leads to a decreased cell viability and a downregulation of heat-shock proteins (HSPs) expression. HSPs expression is normally increased after insufficient temperature elevation or heating duration which can lead to, increased tumor recurrence by enhancing tumor cell viability and imparting resistance to following chemotherapy or hyperthermia therapy (80,81). In a recent study from 2013, Chu *et al*. (82) demonstrated that activated bamboo carbon nanoparticles (BNAC) have the potential to be used in high efficiency cancer phototherapy. In an *in vitro* experiment human lung cancer cells (H-1299) were covered with different BNAC solutions and then irradiated for 20 min with a 655 nm cw laser (0.5 W/cm^2, spot area 5 mm × 8 mm) followed by an incubation of one hour. The cells were effectively killed after incubation with the BNAC and irradiation. The same particles combined with a photosensitizer were used in an *in vivo* experiment using the same cancer cells. The mice were divided into two treatment groups: one with tumors smaller than the laser spot size and one with tumors bigger than the laser spot. The same nanoparticles were injected directly into the tumors, which were then irradiated with a 655 nm cw laser for 20 min every 24 hr for 22 days. All tumors from the first treatment-group disappeared completely. Due to the incorporated photosensitizer the tumors from the second treatment group also showed an increased growth inhibition. No signs of cytotoxicity could be detected in any of the cases.

For tumors deep within the body MWCNTs might have one disadvantage due to the difficulty of administration. Because of their size and without any surface modification, it is very difficult to obtain a sufficient concentration of the nanotubes to to reach the high temperatures necessary for PTT. However, all of these experiments show that besides the typical noble metal nanoparticles also alternative particles, like carbon nanotubes or BNAC have the potential to be used in photothermal cancer therapy.

Other nanoparticles

Besides the AuNPs, liposomes or carbon nanoparticles, multiple other nanoparticles for light triggered therapy have also been proposed.

Jin *et al*., 2013 (83) showed in recent studies, that the use of a nanostructured porphyrin assembly (porphysomes) was successful in the ablation of hypoxic tumors. Porphysomes are self-assembled from porphyin lipids into liposome-like nanoparticles (~100 nm in diameter). Due to the high amount of particles per porphysom (>80,000) porphysomes can absorb the light with extremely high efficiency. The packing density induces self-quenching porphyrin excited states in which the absorbed light energy is released as heat. Monomeric porphyrins can be used as photosensitizers working in a singlet oxygen generating mechanism whereas the assembled porphyrin lipids can be used for PTT (*Figure 5*). This creates the opportunity to directly compare monomeric porphyrin and porphysomes *in vivo*.

The same dose of Photofrin®, an FDA approved porphyrin photosensitizer, and porphysomes were injected *in vivo* into human epidermoid carcinoma (KB) tumor-bearing mice. The mice had two tumors, one of which was kept under hypoxic and the other under hyperoxic conditions to have a better comparison of biodistribution. PDT was performed with a cw 633 nm laser (200 mW, spotsize 9 mm in diameter)

© Pioneer Bioscience Publishing Company. All rights reserved.

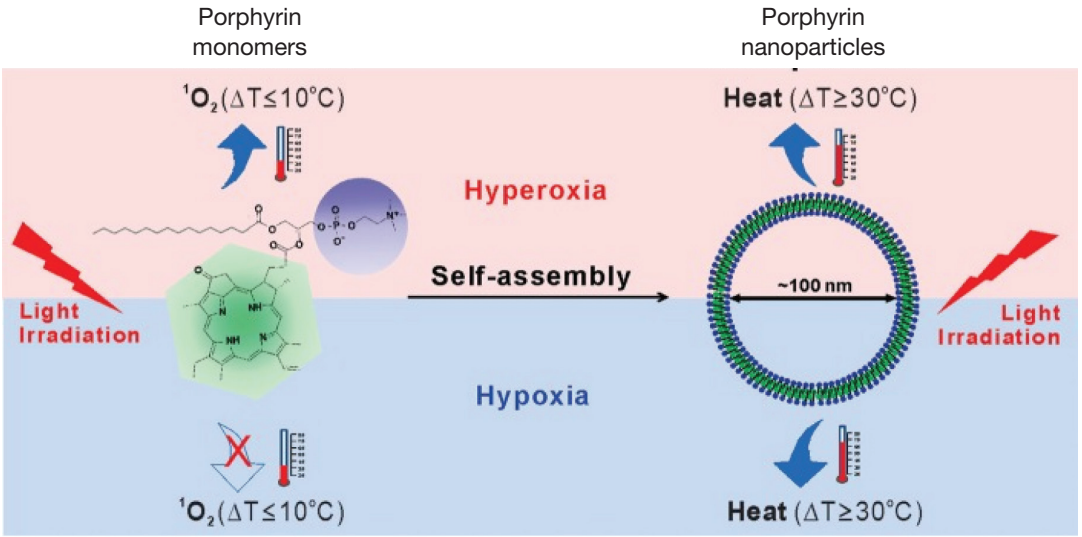

Figure 5 Schematic illustration of the rational design of Porphyrin nanoparticles [Reproduced with permission (83), Copyright © American Chemical Society, 2013]

for 318 seconds. PTT was performed with a cw 671 nm laser (200 mW output, spot size 9 mm) for 85 seconds. The total laser dose for Photofrin® (PDT) and porphysomes (PDT and PTT) was 100 J/cm^2. Only the PTT with porphysomes damaged the hypoxic tumors effectively and led to a survival rate of the mice of 80% after 50 days. The unique properties of these complexes require further investigation but offer a good possibility to treat hypoxic tumors. Nanoparticle formulations of PDT agents are in their infancy and currently limited to ~650 nm excitation. It is expected that photosensitizers excitable in NIR region will be formulated as nanoparticles, however none have been reported yet.

Apart from light in visible and NIR wavelengths, electromagnetic radiation with much longer wavelengths, i.e., radiofrequency (RF) or microwave radiation is also effective for thermally ablative treatment of cancer. Metal nanoparticles are effective converters of RF energy into heat as well, and numerous variants have been reported. (84-87) In particular gold nanospheres have proven to be effective RF triggered thermal therapeutic agents, as they substantially increase RF absorption cross-sections upon deposition in tumor tissue (56).

Modulation through magnetic field

While tremendous progress has been made in the field of light triggered nanoparticle therapies, they are constrained by tissue depth penetration of light, which is limited to a few centimeters, even for higher penetrating NIR wavelengths. Magnetic fields can be applied over clinical spatial regimes, and thus promise non-invasive control of therapy through human bodies. Magnetic nanoparticles (MNP) show the potential to work as a contrast agent for MRI or colloidal mediators for cancer treatment with magnetic hyperthermia (*Figure 6*).

The first reported medical use of magnetite powder for internal application came from the Egyptian physician and philosopher Avicenna in the 10th century A.D. (85). In recent years the focus for the use of MNP has shifted to sophisticated applications, like MRI or magnetic field induced hyperthermia to treat cancer (89,90).

The origin of magnetic heating via inductive mediators depends on the size and the magnetic properties of the particles (91). Although pure single-domain particles of any size can exist in theory, for most ferromagnets a state of quasi-uniformity of magnetization is achieved only when the diameter of the particle is in-between 10-100 nm. The size range is bounded below by the transition to superparamagnetism and above by formation of multiple magnetic domains. In multi-domain ferro- or ferri-magnetic materials, heating occurs due to the hysteresis loss. Large particles contain several sub-domains and every sub-domain has its definite magnetization direction. When exposed to a magnetic field, the domains with magnetization along the magnetic field axis grow and the

© Pioneer Bioscience Publishing Company. All rights reserved.

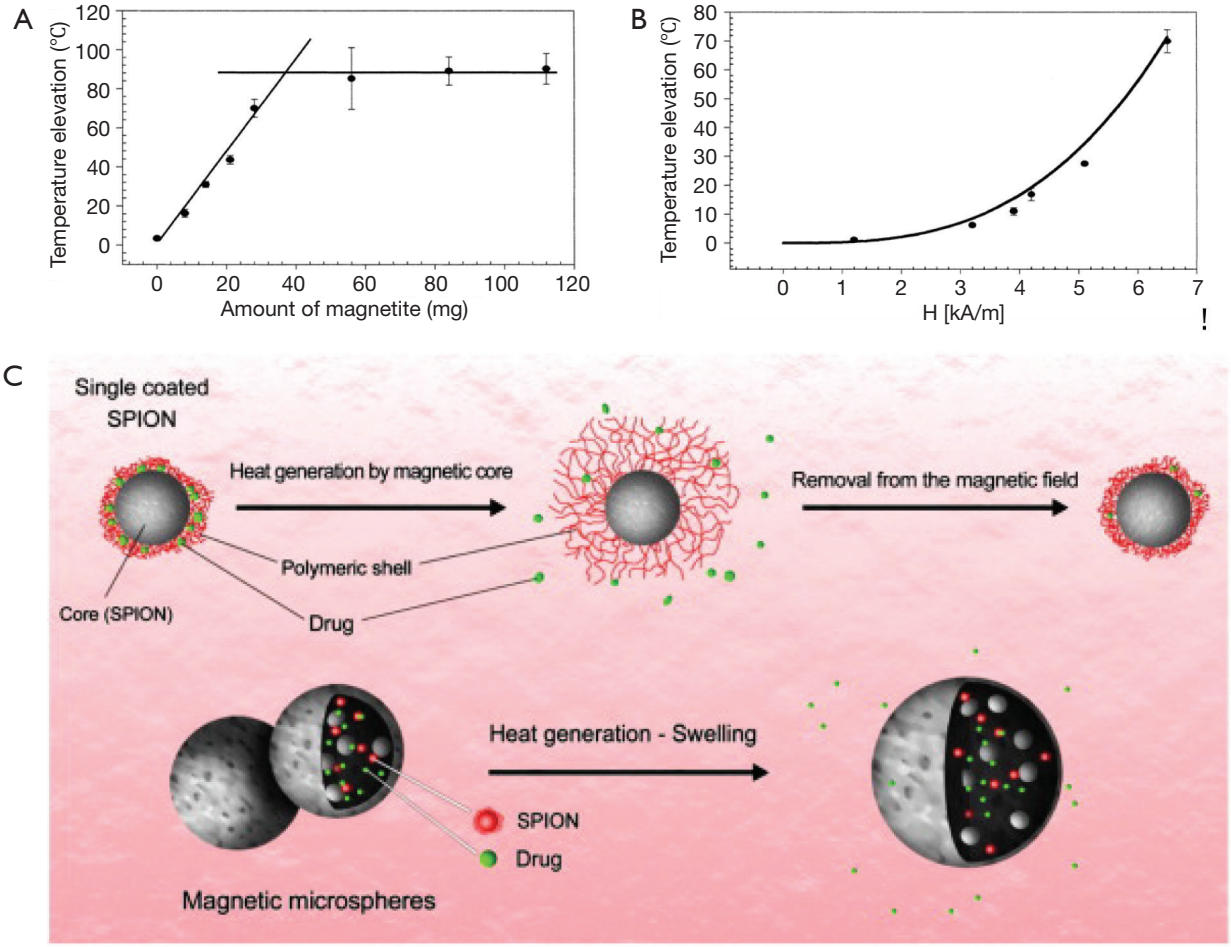

Figure 6 A. Graph of calculated (line) and experimental (•) values of temperature elevation as a function of magnetite mass in breast tissue after an exposure time of 2 minutes. The functional dependency for sample 6 magnetite masses of up to 28 mg is calculated as follows: $\Delta T = 2.31\ M$, with $r^2 = 0.97$, where M is the mass of magnetite and ΔT is the temperature elevation; B. Graph of calculated (line) and experimental (•) values of temperature elevation as a function of magnetic field amplitude in breast tissue after an exposure time of 2 minutes. The functional dependency is calculated as follows: $\Delta T = 0.26\ ℃/(kA/m)^3\ H^3$, with $r^2 = 0.95$, where ΔT is the temperature elevation and H is the magnetic field amplitude [Reproduced with permission (86), Copyright © Radiological Society of North America, 2001]; C. Schematic of magnetic hyperthermia therapy and drug release from super-paramagnetic iron-oxide nanoparticles [Reproduced with permission (88), Copyright © Elsevier, 2011]

others shrink, called "domain wall displacements" (92). This phenomenon is irreversible and materials are said to exhibit "hysteresis behavior" and produce heat under an alternating current (AC) magnetic field. Because of the lack of domain walls in single-domain particles the heat doesn't occur due to hysteresis loss. An externally applied AC magnetic field delivers energy and assists magnetic moments in rotating and overcoming the energy barrier. This energy is dissipated when the particle moment relaxes to its equilibrium orientation (Néel relaxation) (93). Because of these reasons, Fe_3O_4 nanoparticles have the ability to be used as both diagnostic and therapeutic agents. Oscillating magnetic fields (~kHz-MHz) applied to MNP result in the generation of heat, which can increase local temperature to produce hyperthermic effects. One major problem in magnetic hyperthermia is that inductively-coupled magnetic fields to produce heat require a high concentration of Fe_3O_4, which can be difficult to achieve in tumors following systemic delivery. A second related problem is the difficulty in restricting Fe_3O_4 particles only to tumor regions to

© Pioneer Bioscience Publishing Company. All rights reserved.

severe off-target effects, since the applied AC magnetic field affects the whole body (85). A potential solution to these problems is provided by superparamagnetic nanoparticles (SPIONs), which normally have a size <10 nm. SPIONs can leak from the vasculature into normal tissue or be cleared via the renal clearance system and the RES (94,95) which leads to a lower uptake of SPIONs into the tumor. But by clustering the SPIONs in tumors post i.v. delivery, Hayashi *et al*., 2013 (96) could enhance MRI contrast, inhibit tumor growth via magnetic hyperthermia treatment (MHT) and also reduce the needed field force for the AC magnetic field, due to the increased relaxivity and the specific absorption rate of SPION clusters. The clusters were modified with PEG and folic acid for both better biocompatibility and to promote their accumulation in the tumor. 24 hr after i.v. injection into tumor-bearing mice an accumulation into the tumor tissue was observed via enhanced MRI contrast. Mice were placed in an AC magnetic field with a field force of H =8 kA/m and f =230 kHz (Hf =1.8×10^9 A/m*s) for 20 min. Treated tumors experienced a higher temperature than the surrounding tissue. 35 days after treatment the treated tumors had just one-tenth of the volume of the untreated tumors. 12 weeks after treatment all treated mice were alive whereas the untreated mice died after 8 weeks.

This study gives reason for hope to use SPION particles for detection and treatment of multiple myeloma using MRI and MHT. SPION particles didn't show any sign of hepatotoxicity or nephrotoxicity. However, the therapeutic use of MNPs is limited due to their insufficient local accumulation (97).

Modulation through ultrasound

Ultrasound imaging devices are ubiquitous in clinics. The wide penetration, low cost, and low safety concerns with ultrasound technology present a promising avenue for modulating nanoparticle mediated treatments, but the field has made limited progress due to lack of sufficient advancements in nanoparticles engineered to efficiently absorb sonic energy. Ultrasound modulation for cancer treatment is mostly used to enhance drug uptake into the tumor tissue. The distribution of labeled nanoparticles and cancer drugs into tumor tissue depends on several factors like water solubility, nanoparticle size, toxicity effects (local or systemic), tumor hemoperfusion and vasculature permeability. To overcome the water solubility problem cancer drugs, e.g., docetaxel, were often covered with Tween80, which tends to induce allergic reactions (98). Newer studies showed that encapsulation of the drugs into polymeric micelles in combination with ultrasound treatment can overcome the solubility problem as well as increase the drug accumulation in the tumor which directly leads to a decrease of the concentration of free drugs in the system (fewer side effects on healthy tissue). Ultrasound shows a number of attractive properties as a drug delivery modality. It can be directed precisely to the tumor site, even if the tumor is located deep inside the body, either by intraluminal, laparoscopic or percutaneous minimal invasive application or for excorporal sonication the transducer just needs contact with a water-based gel (e.g., ultrasound during pregnancy). The transmission of ultrasonic waves in biological tissues produces thermal effects, acoustic cavitation, mechanical effects and other helpful modifications that improve anticancer effects (99,100). Increased tissue temperature leads to a higher vasculature and cell permeability and therefore a better uptake of drugs into the tumor. Nano- and microbubbles consisting of different combinations of lipids (101) and containing atmospheric air or gas have been proposed for ultrasound mediated therapy (102,103). Due to the leaky tumor vasculature drug loaded nanobubbles and micelles are able to excavate into the tumor, and the tumor accumulation is enhanced when ultrasound is applied. Ultrasound treatment causes the nanobubbles to coalesce and form microbubbles, which are even better echogenic particles. The applied ultrasound provokes the drug-loaded micelles to break and to release the anticancer drug into the tumor tissue. While high-intensity-focused ultrasound (HIFU) is also used directly in cancer treatment, for the ablation of prostate, kidney or uterine tumors, the technique has not been combined with nanoparticles. Currently, the ablative HIFU techniques show a number of problems, like precise control of heat deposition due to patient movement and breathing during the treatment (102) and nanoparticle mediated energy deposition can potentially improve the therapy delivery accuracy.

Conclusions

As described in the previous section, externally modulated theranostic nanoparticles are rapidly advancing and have been validated for cancer therapy in multiple pre-clinical models (104,105). External control on therapy delivery from nanoparticles further enhances the tumor specific action, and reduces off-target effects of frequently morbid cancer therapies. The non-ionizing nature of optical/

© Pioneer Bioscience Publishing Company. All rights reserved.

magnetic or ultrasound energy inputs employed for most of the emerging methods further reduces safety concerns. Nanoparticles have been FDA approved as therapy delivery vehicles for more than 15 years, but only passive liposomes have seen widespread clinical translation. Multi-functional externally modulated nanoparticles are expected to face unique challenges, due to the complexity of treatment strategies and the involvement of an external stimulation device. Only GNS have undergone pilot clinical trials as of now. Further challenges for theranostic nanoparticles involve safety and toxicity concerns arising from high reactive surface to volume ratio, and unclear degradation and clearance mechanisms. While many external field modulated nanoparticle embodiments have been validated in cancer models, even pilot clinical trials require significant investment of resources in scaling up the production to produce hundreds of liters of injectables, with well calibrated properties. Apart from achieving constancy in physio-chemical attributes of size, shape, and surface functionalization, externally modulated nanoparticles need to achieve a constant and calibrated response to the applied external field energies for standard treatment protocols to be possible. Standardized tests for nanoparticle safety and efficacy are under development, and progress on unified standards is slow because of the variety of possible nanoparticle therapies. At NIH, NCI's Nanotechnology Characterization Laboratory (http://ncl.cancer.gov) is developing standards for nanoparticle assessment in collaboration with the FDA. As the standards evolve and early phase clinical trials succeed, larger pharmaceutical concerns and medical device manufacturers are expected to step in with capital investments needed to push externally modulated nanoparticles for widespread clinical use. The next two decades will witness exciting and rapid strides in the transition of theranostic nanoparticles from academic laboratories to clinics.

Acknowledgements

Cordula Urban, Heather Charron, and Amit Joshi were supported by NIH grants R01 CA 151962 and U01 CA 151886.
Disclosure: The authors declare no conflict of interest.

References

1. Schipper ML, Iyer G, Koh AL, et al. Particle size, surface coating, and PEGylation influence the biodistribution of quantum dots in living mice. Small 2009;5:126-34.
2. Torchilin VP. Targeted pharmaceutical nanocarriers for cancer therapy and imaging. AAPS J 2007;9:E128-47.
3. Liong M, Lu J, Kovochich M, et al. Multifunctional inorganic nanoparticles for imaging, targeting, and drug delivery. ACS Nano 2008;2:889-96.
4. Hughes JT. The Edwin Smith Surgical Papyrus: an analysis of the first case reports of spinal cord injuries. Paraplegia 1988;26:71-82.
5. Huang X, Jain PK, El-Sayed IH, et al. Plasmonic photothermal therapy (PPTT) using gold nanoparticles. Lasers Med Sci 2008;23:217-28.
6. Sönnichsen C, Franzl T, Wilk T, et al. Drastic reduction of plasmon damping in gold nanorods. Phys Rev Lett 2002;88:077402.
7. Urban AS, Fedoruk M, Horton MR, et al. Controlled nanometric phase transitions of phospholipid membranes by plasmonic heating of single gold nanoparticles. Nano Lett 2009;9:2903-8.
8. Baffou G, Quidant R. Thermo-plasmonics: using metallic nanostructures as nano-sources of heat. Laser & Photonics Reviews 2013;7:171-87.
9. Knight MW, Liu L, Wang Y, et al. Aluminum plasmonic nanoantennas. Nano Lett 2012;12:6000-4.
10. Scholl JA, Koh AL, Dionne JA. Quantum plasmon resonances of individual metallic nanoparticles. Nature 2012;483:421-7.
11. Chan GH, Zhao J, Hicks EM, et al. Plasmonic properties of copper nanoparticles fabricated by nanosphere lithography. Nano Letters 2007;7:1947-52.
12. Luther JM, Jain PK, Ewers T, et al. Localized surface plasmon resonances arising from free carriers in doped quantum dots. Nat Mater 2011;10:361-6.
13. Jain PK, Huang X, El-Sayed IH, et al. Review of some interesting surface plasmon resonance-enhanced properties of noble metal nanoparticles and their applications to biosystems. Plasmonics 2007;2:107-18.
14. Huang X, Jain PK, El-Sayed IH, et al. Gold nanoparticles: interesting optical properties and recent applications in cancer diagnostics and therapy. Nanomedicine (Lond) 2007;2:681-93.
15. Nance EA, Woodworth GF, Sailor KA, et al. A dense poly (ethylene glycol) coating improves penetration of large polymeric nanoparticles within brain tissue. Sci Transl Med 2012;4:149ra119.
16. Bardhan R, Chen W, Bartels M, et al. Tracking of multimodal therapeutic nanocomplexes targeting breast cancer in vivo. Nano Lett 2010. [Epub ahead of print].

© Pioneer Bioscience Publishing Company. All rights reserved.

17. Patra CR, Bhattacharya R, Wang E, et al. Targeted delivery of gemcitabine to pancreatic adenocarcinoma using cetuximab as a targeting agent. Cancer Res 2008;68:1970-8.
18. Dickerson EB, Dreaden EC, Huang X, et al. Gold nanorod assisted near-infrared plasmonic photothermal therapy (PPTT) of squamous cell carcinoma in mice. Cancer Lett 2008;269:57-66.
19. Balasubramanian SK, Jittiwat J, Manikandan J, et al. Biodistribution of gold nanoparticles and gene expression changes in the liver and spleen after intravenous administration in rats. Biomaterials 2010;31:2034-42.
20. Klien K, Godnic-Cvar J. Genotoxicity of metal nanoparticles: focus on in vivo studies. Arh Hig Rada Toksikol 2012;63:133-45.
21. Li JL, Wang L, Liu XY, et al. In vitro cancer cell imaging and therapy using transferrin-conjugated gold nanoparticles. Cancer Lett 2009;274:319-26.
22. Weissleder R. A clearer vision for in vivo imaging. Nat Biotechnol 2001;19:316-7.
23. Turkevich J, Stevenson PC, Hillier J. A study of the nucleation and growth processes in the synthesis of colloidal gold. Discuss Faraday Soc 1951;11:55-75.
24. Enustun BV, Turkevich J. Coagulation of colloidal gold. J Am Chem Soc 1963;85:3317-28.
25. Turkevich J. Colloidal gold. Part I. Gold Bulletin 1985;18:86-91.
26. Kimling J, Maier M, Okenve B, et al. Turkevich method for gold nanoparticle synthesis revisited. J Phys Chem B 2006;110:15700-7.
27. Afifi MM, El Sheikh SM, Abdelsalam MM, et al. Therapeutic efficacy of plasmonic photothermal nanoparticles in hamster buccal pouch carcinoma. Oral Surg Oral Med Oral Pathol Oral Radiol 2013;115:743-51.
28. Mendoza-Nava H, Ferro-Flores G, Ocampo-García B, et al. Laser heating of gold nanospheres functionalized with octreotide: in vitro effect on HeLa cell viability. Photomed Laser Surg 2013;31:17-22.
29. Shao J, Griffin RJ, Galanzha EI, et al. Photothermal nanodrugs: potential of TNF-gold nanospheres for cancer theranostics. Sci Rep 2013;3:1293.
30. Faber DJ, Mik EG, Aalders MC, et al. Light absorption of (oxy-)hemoglobin assessed by spectroscopic optical coherence tomography. Opt Lett 2003;28:1436-8.
31. Foss CA, Hornyak GL, Stockert JA, et al. Optically transparent nanometal composite membranes. Adv Mater 1993;5:135-7.
32. Jana NR, Gearheart L, Murphy CJ. Seed-mediated growth approach for shape-controlled synthesis of spheroidal and rod-like gold nanoparticles using a surfactant template. Adv Mater 2001;13:1389-93.
33. Huang X, El-Sayed IH, El-Sayed MA. Applications of gold nanorods for cancer imaging and photothermal therapy. Methods Mol Biol 2010;624:343-57.
34. Gans R. Über die Form ultramikroskopischer Silberteilchen. Annalen der Physik 1915;352:270-84.
35. Ali MR, Snyder B, El-Sayed MA. Synthesis and optical properties of small Au nanorods using a seedless growth technique. Langmuir 2012;28:9807-15.
36. Alkilany AM, Thompson LB, Boulos SP, et al. Gold nanorods: their potential for photothermal therapeutics and drug delivery, tempered by the complexity of their biological interactions. Adv Drug Deliv Rev 2012;64:190-9.
37. Huang X, El-Sayed IH, Qian W, et al. Cancer cell imaging and photothermal therapy in the near-infrared region by using gold nanorods. J Am Chem Soc 2006;128:2115-20.
38. Durr NJ, Larson T, Smith DK, et al. Two-photon luminescence imaging of cancer cells using molecularly targeted gold nanorods. Nano Lett 2007;7:941-5.
39. Rosi NL, Mirkin CA. Nanostructures in biodiagnostics. Chem Rev 2005;105:1547-62.
40. Zhang Z, Wang J, Chen C. Gold nanorods based platforms for light-mediated theranostics. Theranostics 2013;3:223-38.
41. Didychuk CL, Ephrat P, Chamson-Reig A, et al. Depth of photothermal conversion of gold nanorods embedded in a tissue-like phantom. Nanotechnology 2009;20:195102.
42. Petrova H, Perez Juste J, Pastoriza-Santos I, et al. On the temperature stability of gold nanorods: comparison between thermal and ultrafast laser-induced heating. Phys Chem Chem Phys 2006;8:814-21.
43. Khalavka Y, Ohm C, Sun L, et al. Enhanced thermal stability of gold and silver nanorods by thin surface layers. J Phys Chem C 2007;111:12886-9.
44. Halas N. The optical properties of nanoshells. Opt Photon News 2002;13:26-30.
45. Radloff C, Halas NJ. Enhanced thermal stability of silica-encapsulated metal nanoshells. Appl Phys Lett 2001;79:674-6.
46. Hirsch LR, Stafford RJ, Bankson JA, et al. Nanoshell-mediated near-infrared thermal therapy of tumors under magnetic resonance guidance. Proc Natl Acad Sci U S A 2003;100:13549-54.
47. Loo C, Lin A, Hirsch L, et al. Nanoshell-enabled photonics-based imaging and therapy of cancer. Technol Cancer Res Treat 2004;3:33-40.

© Pioneer Bioscience Publishing Company. All rights reserved.

48. Bardhan R, Lal S, Joshi A, et al. Theranostic nanoshells: from probe design to imaging and treatment of cancer. Acc Chem Res 2011;44:936-46.
49. Lal S, Clare SE, Halas NJ. Nanoshell-enabled photothermal cancer therapy: impending clinical impact. Acc Chem Res 2008;41:1842-51.
50. Link S, El-Sayed MA. Size and temperature dependence of the plasmon absorption of colloidal gold nanoparticles. J Phys Chem B 1999;103:4212-7.
51. Nikoobakht B, El-Sayed MA. Preparation and growth mechanism of gold nanorods (NRS) using seed-mediated growth method. Chem Mater 2003;15:1957-62.
52. Park K, Lee S, Kang E, et al. New generation of multifunctional nanoparticles for cancer imaging and therapy. Adv Funct Mater 2009;19:1553-66.
53. Sikdar D, Rukhlenko ID, Cheng W, et al. Effect of number density on optimal design of gold nanoshells for plasmonic photothermal therapy. Biomed Opt Express 2013;4:15-31.
54. Gad SC, Sharp KL, Montgomery C, et al. Evaluation of the toxicity of intravenous delivery of auroshell particles (gold-silica nanoshells). Int J Toxicol 2012;31:584-94.
55. Loo C, Lowery A, Halas NJ, et al. Immunotargeted nanoshells for integrated cancer imaging and therapy. Nano Letters 2005;5:709-11.
56. Gannon CJ, Patra CR, Bhattacharya R, et al. Intracellular gold nanoparticles enhance non-invasive radiofrequency thermal destruction of human gastrointestinal cancer cells. J Nanobiotechnology 2008;6:2.
57. Bardhan R, Chen W, Perez-Torres C, et al. Nanoshells with targeted simultaneous enhancement of magnetic and optical imaging and photothermal therapeutic response. Adv Funct Mater 2009;19:3901-9.
58. Sershen SR, Westcott SL, Halas NJ, et al. Temperature-sensitive polymer-nanoshell composites for photothermally modulated drug delivery. J Biomed Mater Res 2000;51:293-8.
59. Van de Broek B, Devoogdt N, D'Hollander A, et al. Specific cell targeting with nanobody conjugated branched gold nanoparticles for photothermal therapy. ACS Nano 2011;5:4319-28.
60. Wang Y, Black KCL, Luehmann H, et al. Comparison study of gold nanohexapods, nanorods, and nanocages for photothermal cancer treatment. ACS Nano 2013;7:2068-77.
61. Chen J, Wang D, Xi J, et al. Immuno gold nanocages with tailored optical properties for targeted photothermal destruction of cancer cells. Nano Lett 2007;7:1318-22.
62. Chen W, Bardhan R, Bartels M, et al. A molecularly targeted theranostic probe for ovarian cancer. Mol Cancer Ther 2010;9:1028-38.
63. Melancon MP, Lu W, Yang Z, et al. In vitro and in vivo targeting of hollow gold nanoshells directed at epidermal growth factor receptor for photothermal ablation therapy. Molec Cancer Ther 2008;7:1730-9.
64. Lu W, Melancon MP, Xiong C, et al. Effects of photoacoustic imaging and photothermal ablation therapy mediated by targeted hauns in an orthotopic mouse xenograft model of glioma. Cancer Res 2011;71:6116-21.
65. Sułkowski WW, Pentak D, Nowak K, et al. The influence of temperature, cholesterol content and pH on liposome stability. J Mol Struct 2005;744-747:737-47.
66. Laouini A, Jaafar-Maalej C, Limayem-Blouza I, et al. Preparation, characterization and applications of liposomes: state of the art. J Colloid Sci Biotech 2012;1:147-68.
67. Needham D, Dewhirst MW. The development and testing of a new temperature-sensitive drug delivery system for the treatment of solid tumors. Adv Drug Deliv Rev 2001;53:285-305.
68. Shum P, Kim JM, Thompson DH. Phototriggering of liposomal drug delivery systems. Adv Drug Deliv Rev 2011;53:273-84.
69. Regen SL, Singh A, Oehme G, et al. Polymerized phosphatidyl choline vesicles. Stabilized and controllable time-release carriers. Biochem Biophys Res Commun 1981;101:131-6.
70. Rhodes DG, Blechner SL, Yager P, et al. Structure of polymerizable lipid bilayers. I--1,2-bis(10,12-tricosadiynoyl)-sn-glycero-3-phosphocholine, a tubule-forming phosphatidylcholine. Chem Phys Lipids 1988;49:39-47.
71. Puri A, Loomis K, Smith B, et al. Lipid-based nanoparticles as pharmaceutical drug carriers: from concepts to clinic. Crit Rev Ther Drug Carrier Syst 2009;26:523-80.
72. Smith B, Lyakhov I, Loomis K, et al. Hyperthermia-triggered intracellular delivery of anticancer agent to HER2(+) cells by HER2-specific affibody (ZHER2-GS-Cys)-conjugated thermosensitive liposomes (HER2(+) affisomes). J Control Release 2011;153:187-94.
73. Löfblom J, Feldwisch J, Tolmachev V, et al. Affibody molecules: engineered proteins for therapeutic, diagnostic and biotechnological applications. FEBS Lett 2010;584:2670-80.
74. Yavlovich A, Singh A, Tarasov S, et al. Design of liposomes containing photopolymerizable phospholipids

© Pioneer Bioscience Publishing Company. All rights reserved.

for triggered release of contents. J Therm Anal Calorim 2009;98:97-104.
75. Jackson JD. eds. Classical electrodynamics. 3rd Edition. Wiley, 1999.
76. Torti SV, Byrne F, Whelan O, et al. Thermal ablation therapeutics based on CN(x) multi-walled nanotubes. Int J Nanomedicine 2007;2:707-14.
77. Sun X, Yu RQ, Xu GQ, et al. Broadband optical limiting with multiwalled carbon nanotubes. Appl Phys Lett 1998;73:3632-4.
78. Burke A, Ding X, Singh R, et al. Long-term survival following a single treatment of kidney tumors with multiwalled carbon nanotubes and near-infrared radiation. Proc Natl Acad Sci U S A 2009;106:12897-902.
79. Fisher JW, Sarkar S, Buchanan CF, et al. Photothermal response of human and murine cancer cells to multiwalled carbon nanotubes after laser irradiation. Cancer Res 2010;70:9855-64.
80. Madersbacher S, Grobl M, Kramer G, et al. Regulation of heat shock protein 27 expression of prostatic cells in response to heat treatment. Prostate 1998;37:174-81.
81. Gibbons NB, Watson RW, Coffey RN, et al. Heat-shock proteins inhibit induction of prostate cancer cell apoptosis. Prostate 2000;45:58-65.
82. Chu M, Peng J, Zhao J, et al. Laser light triggered-activated carbon nanosystem for cancer therapy. Biomaterials 2013;34:1820-32.
83. Jin CS, Lovell JF, Chen J, et al. Ablation of hypoxic tumors with dose-equivalent photothermal, but not photodynamic, therapy using a nanostructured porphyrin assembly. Acs Nano 2013;7:2541-50.
84. Cardinal J, Klune JR, Chory E, et al. Non-invasive radiofrequency ablation of cancer targeted by gold nanoparticles. Surgery 2008;144:125-32.
85. Cherukuri P, Glazer ES, Curley SA. Targeted hyperthermia using metal nanoparticles. Adv Drug Deliv Rev 2010;62:339-45.
86. Hilger I, Andrä W, Hergt R, et al. Electromagnetic heating of breast tumors in interventional radiology: in vitro and in vivo studies in human cadavers and mice1. Radiology 2001;218:570-5.
87. Wu X, Zhao F, Rahunen N, et al. A role for microbial palladium nanoparticles in extracellular electron transfer. Angew Chem Int Ed Engl 2011;50:427-30.
88. Laurent S, Dutz S, Hafeli UO, et al. Magnetic fluid hyperthermia: focus on superparamagnetic iron oxide nanoparticles. Adv Colloid Interface Sci 2011;166:8-23.
89. Mornet S, Vasseur S, Grasset F, et al. Magnetic nanoparticle design for medical diagnosis and therapy. J Mater Chem 2004;14:2161-75.
90. Ahmed N, Michelin-Jamois M, Fessi H, et al. Modified double emulsion process as a new route to prepare submicron biodegradable magnetic/polycaprolactone particles for in vivo theranostics. Soft Matter 2012;8:2554-64.
91. Andrä WN. eds. Magnetism in medicine: a handbook. 1 edit. Hannes, 1998.
92. Stein FU, Bocklage L, Weigand M, et al. Time-resolved imaging of nonlinear magnetic domain-wall dynamics in ferromagnetic nanowires. Sci Rep 2013;3:1737.
93. Jordan A, Wust P, Fahling H, et al. Inductive heating of ferrimagnetic particles and magnetic fluids: physical evaluation of their potential for hyperthermia. Int J Hyperthermia 1993;9:51-68.
94. Choi HS, Liu W, Misra P, et al. Renal clearance of quantum dots. Nat Biotechnol 2007;25:1165-70.
95. Maki S, Konno T, Maeda H. Image enhancement in computerized tomography for sensitive diagnosis of liver cancer and semiquantitation of tumor selective drug targeting with oily contrast medium. Cancer 1985;56:751-7.
96. Hayashi K, Nakamura M, Sakamoto W, et al. Superparamagnetic nanoparticle clusters for cancer theranostics combining magnetic resonance imaging and hyperthermia treatment. Theranostics 2013;3:366-76.
97. Liu HL, Hua MY, Yang HW, et al. Magnetic resonance monitoring of focused ultrasound/magnetic nanoparticle targeting delivery of therapeutic agents to the brain. Proc Natl Acad Sci U S A 2010;107:15205-10.
98. van Zuylen L, Verweij J, Sparreboom A. Role of formulation vehicles in taxane pharmacology. Invest New Drugs 2001;19:125-41.
99. Lentacker I, Geers B, Demeester J, et al. Tumor cell killing efficiency of doxorubicin loaded microbubbles after ultrasound exposure. J Control Release 2010;148:e113-4.
100. Suzuki R, Namai E, Oda Y, et al. Cancer gene therapy by IL-12 gene delivery using liposomal bubbles and tumoral ultrasound exposure. J Control Release 2010;142:245-50.
101. Husseini GA, Pitt WG. Micelles and nanoparticles for ultrasonic drug and gene delivery. Adv Drug Deliv Rev 2008;60:1137-52.
102. Rapoport N, Gao Z, Kennedy A. Multifunctional nanoparticles for combining ultrasonic tumor imaging and targeted chemotherapy. J Natl Cancer Inst 2007;99:1095-106.
103. Figueiredo M, Esenaliev R. PLGA nanoparticles for

© Pioneer Bioscience Publishing Company. All rights reserved.

ultrasound-mediated gene delivery to solid tumors. J Drug Deliv 2012;2012:767839.
104. Ahmed N, Fessi H, Elaissari A. Theranostic applications of nanoparticles in cancer. Drug Discovery Today 2012;17:928-34.
105. Rajaram S, Bhujbal P, Slipper IJ, et al. Prostate cancer targeting with 7E11-C5.3-CdS bioconjugated quantum dots. J Colloid Sci Biotech 2013;2:34-9.

Cite this article as: Urban C, Urban AS, Charron H, Joshi A. Externally modulated theranostic nanoparticles. Transl Cancer Res 2013;2(4):292-308. doi: 10.3978/j.issn.2218-676X.2013.08.05

© Pioneer Bioscience Publishing Company. All rights reserved.